Journal of ELECTRICAL ENGINEERING, VOL 69 (2018), NO3, 212–218

Emulator of harmonic distortion of bias port of the Mach-Zehnder intensity modulator

Jiri Svarny *

The paper deals with the design of an analog circuit to substitute the role of a real intensity Mach-Zehnder modulator for the preliminary tuning of bias controllers. The proposed circuit has similar harmonic distortion as an electro-optic modulator biased around the quadrature operating point. The designed device utilizes a shaping circuit based on a differential pair of bipolar junction transistors. The harmonic distortion of both the Mach-Zehnder intensity modulator and the differential amplifier are analysed. A method to design the emulating circuit of desired features is described and explained and a the comparison of the measured results to the theory is presented.

K e y w o r d s: circuit emulation, electro-optic modulator, harmonic analysis, harmonic distortion, intensity modulation

1 Introduction

Analog intensity electro-optic modulator of Mach-Zehnder type (MZM) is an usual component of integrated optoelectronics. Its major advantage is the possibility to be implemented in wide-band analog transmission lines. These, externally modulated systems, considerably exceed the limits of the transmission systems based on directly modulated lasers. This is due to achievable modulation depth, bandwidth, optical power of the transmitter and SNR as well. On the other hand, the higher price is a drawback. Considerable amount of the costs is the price of the modulator itself.

The value of the DC bias has substantial influence on behavior of the MZM. In analog transmission systems the modulator is biased to a quadrature point. Thus, the maximum linearity and minimum distortion is achieved. Unfortunately, the intensity MZMs suffer from the drift [1-4].

Due to the drift, the modulator DC bias must be controlled to reach a stable operating point. This is usually done by specialized automatic feedback system. There have been developed a lot of techniques to control the bias voltage of the intensity MZM [4-7]. The most effective methods use the injection of harmonic pilot signal to the modulator bias port and the detection of harmonic components at the modulator output [8-11]. The feedback system is designed to control the DC bias voltage to achieve the desired harmonics at the output.

The design and implementation of analog circuit that emulates harmonic distortion at the output of a real intensity modulator biased in the vicinity of a quadrature point is described below. The proposed analog circuit can be used for safe and cost effective preliminary tests and tuning of the bias controllers. Thus, threat of damage of expansive modulator can be minimized.

2 Harmonic distortion of a modulator

Modern analog intensity modulators have standalone RF port, the bias port and are equipped with integrated monitor photodiode (PD) as well. The PD monitors the output optical power of the modulator. The transfer characteristic of the MZM (*ie* dependency of output optical power P_o on the input voltage V_{in}) is shown in Fig. 1 (red curve). The blue curve represents monitor photodiode current I_{PD}. The V_{+QDC} is DC level that has to be applied to the input of the MZM in order to set-up the positive quadrature point +Quad (desired operating point). The doted curves describe behavior of the MZM under the influence of possible drift.

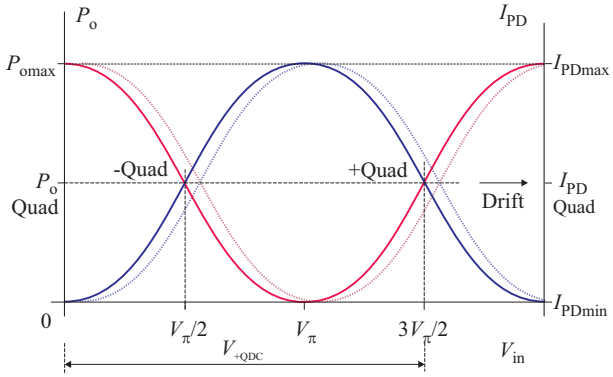

Fig. 1. The transfer chart of the MZM

The signal at the PD monitor port has to be conditioned by an external trans-impedance amplifier (TIA) to obtain the voltage

$$V_{out} = f(V_{in}). \tag{1}$$

University of West Bohemia, Department of Technologies and Measurement, Faculty of Electrical Engineering, Regional Innovation Centre of Electrical Engineering (RICE), Pilsen, Czech Republic, svarny@ket.zcu.cz

DOI: 10.2478/jee-2018–0028, Print (till 2015) ISSN 1335-3632, On-line ISSN 1339-309X

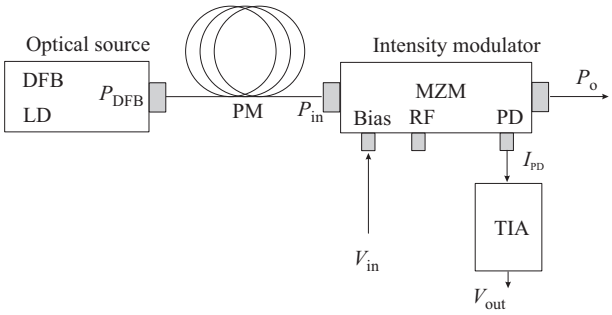

Fig. 2. DFB-MZM-TIA chain – the arrangement to emulate

The configuration in the Fig. 2 can be described by

$$V_{\text{out}} = V_{\text{REF}} - R_{\text{TIA}} S_{\text{PD}} P_{\text{o}} \tag{2}$$

where V_{REF} is the inner reference voltage of the TIA, R_{TIA} is the transimpedance constant of the TIA and S_{PD} is responsivity of the inner PD. In case of driving of the MZM by V_{in} voltage (applied to the bias port) the output optical power of the modulator is

$$\begin{aligned} P_{\text{o}} &= P_{\text{q}} \left[1 + \cos\phi\right], \\ P_{\text{q}} &= \frac{P_{\text{in}} 10^{\frac{\alpha_{\text{dB}}}{10}}}{2}, \quad \phi = \frac{V_{\text{in}}}{V_\pi}\pi \end{aligned} \tag{3}$$

and P_{in} is input optical power of the modulator (*ie* output optical power of the DFB laser), α_{dB} is insertion loss of the modulator, and V_π is the half-wave voltage of the bias port. The output voltage of the TIA is

$$\begin{aligned} V_{\text{out}} &= V_{\text{REF}} - V_\phi \left[1 + \cos\phi\right], \\ V_\phi &= R_{\text{TIA}} S_{\text{PD}} P_{\text{q}}. \end{aligned} \tag{4}$$

Let us consider the driving signal in form

$$V_{\text{in}} = V_{\text{DC}} + V_{\text{AC}} \sin\omega t \tag{5}$$

ie harmonic signal with frequency ω and amplitude V_{AC} superimposed to a DC level V_{DC}. The output voltage V_{out}, can be expressed as

$$\begin{aligned} V_{\text{out}} &= V_{\text{REF}} - V_\phi \\ &- V_\phi \cos\phi_{\text{DC}} \cos(\phi_{\text{AC}} \sin\omega t) \\ &+ V_\phi \sin\phi_{\text{DC}} \sin(\phi_{\text{AC}} \sin\omega t) \end{aligned} \tag{6}$$

$$\phi_{\text{DC}} = \frac{V_{\text{DC}}}{V_\pi}\pi, \quad \phi_{\text{AC}} = \frac{V_{\text{AC}}}{V_\pi}\pi. \tag{7}$$

By means of the Bessel expansion

$$\begin{aligned} \cos(x \sin y) &= J_0(x) + 2 \sum_{k=2,4}^{\infty} J_k(x) \cos ky \\ \sin(x \sin y) &= 2 \sum_{k=1,3}^{\infty} J_k(x) \sin ky \end{aligned} \tag{8}$$

the output voltage V_{out} can be rewritten

$$\begin{aligned} V_{\text{out}} &= V_{\text{REF}} - V_\phi [1 + J_0(\phi_{\text{AC}}) \cos\phi_{\text{DC}} \\ &- 2V_\phi \cos\phi_{\text{DC}} \sum_{k=2,4}^{\infty} J_k(\phi_{\text{AC}}) \cos k\omega t \\ &+ 2V_\phi \sin\phi_{\text{DC}} \sum_{k=1,3}^{\infty} J_k(\phi_{\text{AC}}) \sin k\omega t \end{aligned} \tag{9}$$

summing over even and odds integers respectively.

From (9) the magnitudes of particular harmonic components can be derived.

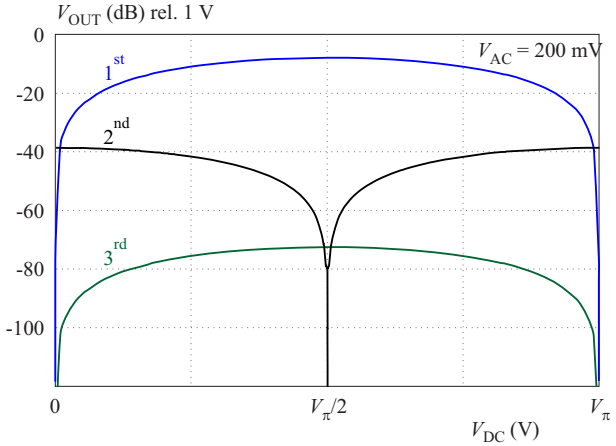

Fig. 3. Dependence of magnitudes of 1st, 2nd and 3rd harmonics on DC bias V_{DC} and TIA output for driving signal $V_{\text{AC}} = 200$ mV

The magnitude of the n^{th} odd and even harmonic component (in dB related to 1 V) are respectively

$$\begin{aligned} V_n &= 20 \log |2V_\phi J_n(\phi_{\text{AC}}) \sin\phi_{\text{DC}}| \\ &\text{for } n \in \langle 1, 3, 5, \ldots \rangle \end{aligned} \tag{10}$$

$$\begin{aligned} V_n &= 20 \log |2V_\phi J_n(\phi_{\text{AC}}) \cos\phi_{\text{DC}}| \\ &\text{for } n \in \langle 2, 4, 6, \ldots \rangle \end{aligned} \tag{11}$$

Dependence of amplitudes of the first three harmonics as a function of bias V_{DC} is in Fig. 3. The calculations for a real parameters of the DFB-MZM-TIA chain equipped with FA20 modulator by Avanex Corp. ($P_{\text{in}} = 21.68$ mW, $\alpha_{\text{dB}} = -3$ dB, $V_\pi = 5.2$ V, $R_{\text{TIA}} = 470$ kΩ, $S_{\text{PD}} = 1.3$ mA/W) were done at $V_{\text{AC}} = 200$ mV.

3 The principle of emulator

The goal was to design a circuit to imitate the nonlinearity of the transfer characteristic of the MZM. Maximum fidelity has been desired around the quadrature point. From mathematical point of view the imitating function should be an approximation in vicinity of the inflexion point of the sine function.

The real-time sampling rate, analog-digital converter (ADC) conversion rate, digital-signal processor calculations time and digital-analog converter (DAC) conversion

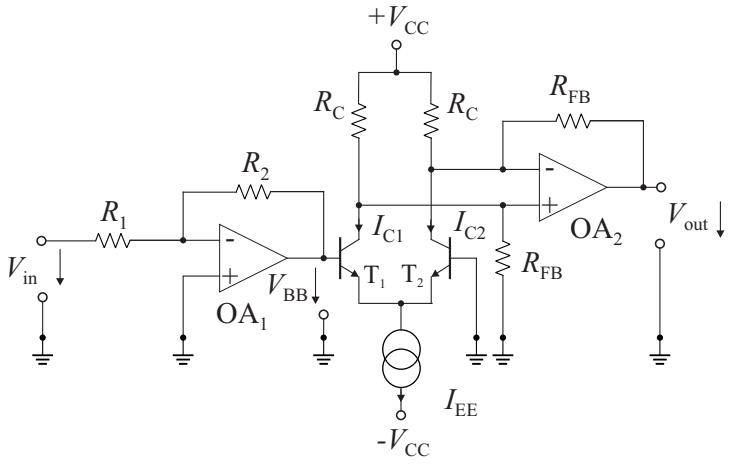

Fig. 4. Simplified core part of the MZM emulator

rate would lead to a significant propagation delay and unwanted phase shift between bias signal and TIA output. The ADC and DAC non-linearity and quantization noise would induce additional problems. That is why an analog shaping technique as a basic emulator concept was chosen. The issue resembles the task of shaping-out the sine function from a triangle waveform [12], [13]. One of the popular and well known shaping techniques is based on use of a differential bipolar junction transistor (BJT) and substitution of the sine function by tanh, see [14-17]. The method is traditionally used in low-frequency function generators. The key part of our emulator is the circuit in Fig. 4.

The collector current difference ΔI_C is in a non-linear relation to the voltage V_{BB}. The non-linearity is described by the function of hyperbolic-tangent (12). Provided the ideal match of both of transistors the V_{T} is the thermal voltage (25.85 mV at 25 °C) and the α_{F} is current gain factor for common base connection (0.98 typically). The I_{EE} is a sum of currents of the emitters (generated by constant current source). From the Shockley equation and the relation between the hyperbolic-tangent and exponential function [16] follows

$$\Delta I_C = I_{C1} - I_{C2} = \alpha_{\mathrm{F}} I_{\mathrm{EE}} \tanh\left(\frac{V_{\mathrm{BB}}}{2V_{\mathrm{T}}}\right) \tag{12}$$

The OA_1 works as a voltage divider with low-impedance output and provides an output/input ratio of G_{in}. The OA_2 works as a transducer of the current difference ΔI_C to the output voltage V_{out}. The transfer function of the circuit is

$$G_{\mathrm{in}} = \frac{V_{\mathrm{BB}}}{V_{\mathrm{in}}} = -\frac{R_2}{R_1} \tag{13}$$

$$V_{\mathrm{out}} = -\psi \tanh \frac{G_{\mathrm{in}} V_{\mathrm{in}}}{2V_{\mathrm{T}}} \quad \text{where} \quad \psi = R_{\mathrm{FB}} \alpha_F I_{\mathrm{EE}}. \tag{14}$$

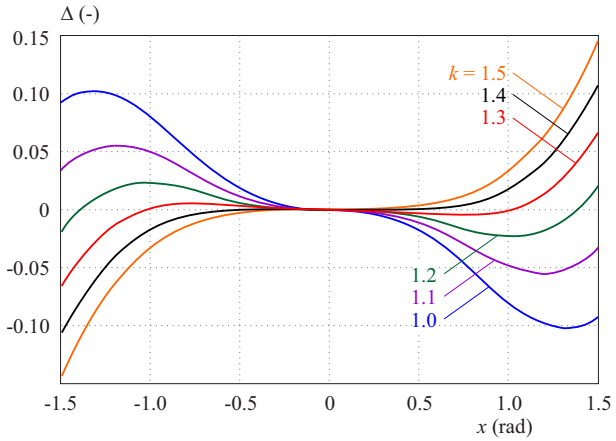

Fig. 5. The influence of k-value to the quality of approximation of $\sin(x)$ function by $k\tanh(x/k)$ function

Stipulation of individual parameters of (14) (R_{FB}, I_{EE}, G_{in}) in order to match the transfer chart of the particular modulator is necessary. Naturally, the substitution is limited to certain area around the origin where the differences are negligible. The goal was to cover range $(-V_\pi/4; V_\pi/4)$ of V_{DC} *ie* (-0.785 rad; 0.785 rad) around quadrature point of the modulator.

The approximation of $\sin(x)$ by $\tanh(x)$ is sufficient for very limited span of x-variable. Much better approximation can be

$$\sin x \cong k \tanh \frac{x}{k}, \tag{15}$$

where k is a real number.

Optimal value of k-parameter is a compromise between effort to cover a wider x-range and an achievable accuracy of the approximation. The influence of k-value to the quality of approximation can be seen in Fig. 5 which shows the error $\Delta = k\tanh(x/k) - \sin x$ for several k-values and x varying from -1.5 rad to +1.5 rad

In the vicinity of the quadrature point the substitution (15) can be well used. Taking into account equations (3) with $x = \phi$ and (14) if we put for argument of tanh function

$$\frac{\phi}{k} = \frac{G_{\mathrm{in}} V_{\mathrm{in}}}{2V_T} \tag{16}$$

the following relation can be directly found

$$G_{\text{in}} = -\frac{2V_T}{kV_\pi}\pi. \tag{17}$$

It is obvious that the perfect match of the functions is ensured in quadrature point only, where

$$\left.\frac{\partial \sin\phi}{\partial\phi}\right|_{\phi=0} = -k\left.\frac{\partial \tanh\left(\frac{\phi}{k}\right)}{\partial\phi}\right|_{\phi=0}. \tag{18}$$

In accordance with Fig. 5 the optimum k-value is expected within the interval (1.3 to 1.5). For given values: $V_\pi = 5.2$ V, and $V_{\text{T}} = 25.85$ mV at 25 °C the G_{in} works out within the interval (-0.024; -0.020). The k-value sets the level of linearization of transfer characteristic of the emulator in vicinity of quadrature point. The set-up of the parameter is closely linked with value of V_π voltage above all. The I_{EE}, R_{FB}, and G_{in} values are linked together and affect each other. In order to let it work, any variation of G_{in} has to be compensated by proper adjustment of I_{EE} and/or R_{FB}.

The exact stipulation of R_{FB}, R_{C}, I_{EE}, and G_{in} values was based on general results of the harmonic analysis of the proposed emulator. Comparison of calculated output spectrum of the emulator with the output spectrum of the mathematical model of real MZM (10), (11) is provided below.

4 Harmonic distortion of the emulator

Considering the basic emulator topology (Fig. 4) and input signal waveform V_{in} (5) the output voltage V_{out} can be expressed as

$$\begin{aligned} &V_{\text{out}} = -\psi \tanh\left[\xi(1+\lambda\sin\omega t)\right], \\ &\text{with:}\quad \xi = G_{\text{in}}\frac{V_{\text{DC}}}{2V_T},\quad \lambda = \frac{V_{\text{AC}}}{V_{\text{DC}}}. \end{aligned} \tag{19}$$

The analytic calculations were simplified by Taylor polynomial approximation limited to the 5^{th} order

$$\tanh(x) \cong x - \frac{x^3}{3} + \frac{2x^5}{15}, \tag{20}$$

yielding

$$\begin{aligned} V_{\text{out}} \simeq -\psi\,[&f_0 + f_1\sin\omega t + \\ &+ f_2\cos 2\omega t - f_3\sin 3\omega t + \\ &+ f_4\cos 4\omega t + f_5\sin 5\omega t], \end{aligned} \tag{21}$$

where

$$\begin{aligned} f_0(\xi,\lambda) &= \xi\left[1-\xi^2(\frac{1}{3}+\frac{\lambda^2}{2}) + \frac{2\xi^4}{15}(1+5\lambda^2+\frac{15\lambda^4}{8})\right], \\ f_1(\xi,\lambda) &= \xi\lambda\left[1-\xi^2(1+\frac{\lambda^2}{4}) + \xi^4(\frac{2}{3}+\lambda^2+\frac{\lambda^4}{12})\right], \\ f_2(\xi,\lambda) &= \xi^3\lambda^2\left[\frac{1}{2} - \frac{\xi^2}{3}(2+\lambda^2)\right], \\ f_3(\xi,\lambda) &= \frac{\xi^3\lambda^3}{12}\left[1-\xi^2(4+\frac{\lambda^2}{2})\right], \\ f_4(\xi,\lambda) &= \frac{\xi^5\lambda^4}{12}, \\ f_5(\xi,\lambda) &= \frac{\xi^5\lambda^5}{120}. \end{aligned}$$

The magnitude of n^{th} harmonic V_n^{out} in dB related to 1 V (for first 5 harmonics) are clearly seen to be determined by $f_n(\xi,\lambda)$, expressions as

$$V_n^{\text{out}} \simeq 20\log|\psi f_n(\xi,\lambda)| \quad \text{for } n \in \langle 1,2,\ldots 5\rangle. \tag{22}$$

5 Implementation

The MAT01AH dual BJT was used to design the differential stage [18]. The main advantage of the device is the almost perfect match of the key parameters of both transistors. The voltage offset (V_{BE}) is 40 μV only and the offset drift is typically 0.5 μV/ °C . The next considerations and calculations were done using $\alpha_{\text{F}} = 0.98$ which is a typical value of current gain for most of the transistors working in common base configuration. The MAT01AH demonstrate best linearity of h_{21e} for emitter currents within the range from 10 nA up to 10 mA. To operate the BJT stage in optimal regime the I_{EE} was chosen in order of hundreds of μA. As the V_{CC} supply rails are ± 5 V, the R_{C} resistors were set-up to 2.4 kΩ. The I_{EE} current and the R_{FB} resistor define the gain of the circuit. The values are in relation of inverse proportionality *ie* an increase of the first one must be compensated by a decrease of the second one and vice versa.

For allowable span of the I_{EE} (100 μA to 1 mA) and assumed interval of k-value (1.3 to 1.5) there is R_{FB} ranging from 3.38 kΩ to 33.8 kΩ. The correct function of the differential stage is limited by the perfect match of corresponding R_{C} to R_{FB} ratios. That is why the R_{FB} value was chosen as the fixed one and I_{EE} and G_{in} values were tuned.

Relations of 1^{st}, 2^{nd} and 3^{rd} harmonics were processed numerically. The goal was to find the optimal value G_{in} to match the emulator equations with the MZM mathematical model. To facilitate the comparison there was supposed the same value of driving signal (200 mV) for mathematical model of the MZM and the emulating circuit as well. In case the MZM is driven by $V_{\text{AC}} = 200$ mV, there can be found -8.076 dB fundamental level and

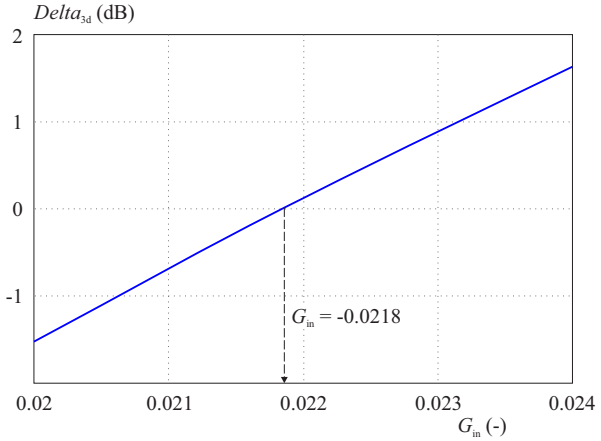

Fig. 6. Stipulation of optimal value of G_{in} based on the fundamental and the 3rd harmonic match

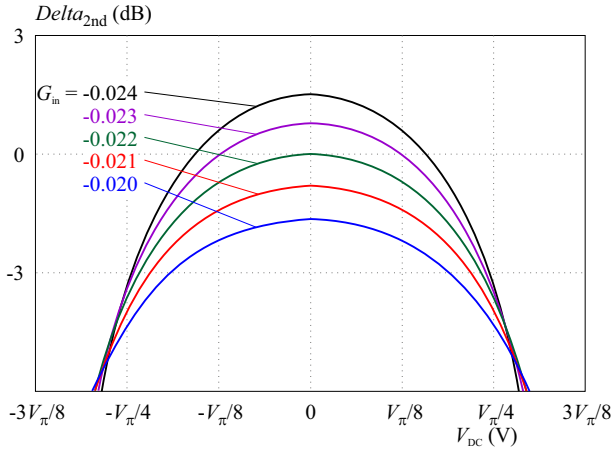

Fig. 7. Optimization of G_{in} regard to the error of 2nd harmonic

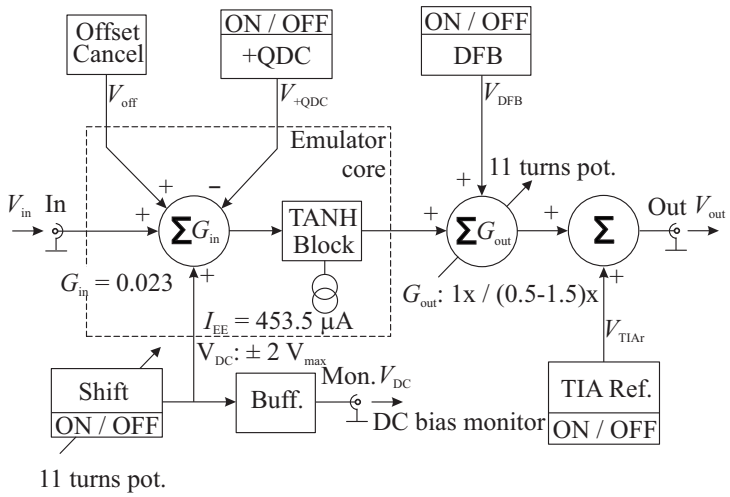

Fig. 8. Block diagram of the emulator

-72.595 dB of 3rd harmonic level at the quadrature point (see Fig. 3). Gradually, there were considered particular values of G_{in} within the predefined interval. Simultaneously, the value I_{EE} was tuned in order to reach the reference level V_1^{out} (-8.076 dB) by (22). Subsequently, the comparison of the 3rd harmonic at the output of the emulator V_3^{out} (22) and the value given by the MZM mathematical model *ie* $V_3 = -72.595dB$ by (10) was done. The difference provided the quadrature point is achieved is shown in Fig. 6.

In accordance with Fig. 6, the target value of the G_{in} should be -0.0218. However, the method reflects the perfect match of the substitute chart with the original one at the quadrature point only. A prospective mismatch of the charts out of the quadrature point is not respected. That is why, there was done additional correction of the G_{in} value.

For particular value of $G_{\text{in}} I_{\text{EE}}$ there were calculated differences in 2nd harmonic as a function of position of operating point. The deviation of 2nd harmonic from that of mathematical model (11) are in Fig. 7.

In regard of 2nd harmonic the zero error at the quadrature point is achieved for G_{in} = -0.022 (similar result as in case of 3rd harmonic error). Nevertheless, the charts in Fig. 7 reveal that the desired value of $|G_{\text{in}}|$should be a little bit higher than 0.022 to ensure better distribution of error in whole the range of V_{DC} $(-V_\pi/4; V_\pi/4)$. The chosen value was G_{in} = -0.023 then.

The calculations revealed the target value of G_{in} and I_{EE}. The value G_{in} = -0.023 is achieved using 0.1% resistors R_1 = 104.3 kΩ (100 kΩ and 4.3 kΩ) and R_2 = 2.4 kΩ, see Fig. 4. The value of I_{EE} = 453.5 µA is controlled by a constant current source. The nonlinearity core part (TANH Block) is accompanied with some additional blocks, see Fig. 8. The additional circuits provide the set-up of the DC offsets of input and output signals respectively. The Offset Cancel block generates V_{off} voltage that is necessary to cancel out the intrinsic offset of the dual BJT stage. Block +QDC generates DC level $V_{+\text{QDC}}$ to achieve positive quadrature point of the MZM. The voltage is subtracted from the input signal V_{in} actually. The V_{DFB} (generated by DFB block) is DC voltage emulating quiescent output level of the MZM in case the modulator is excited by DFB laser. The V_{TIAr} voltage at the output of TIA Ref. block emulates the level of reference voltage of the TIA. Emulation of drift is ensured

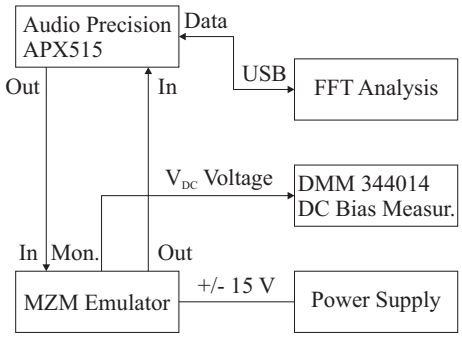

Fig. 9. The emulator verification

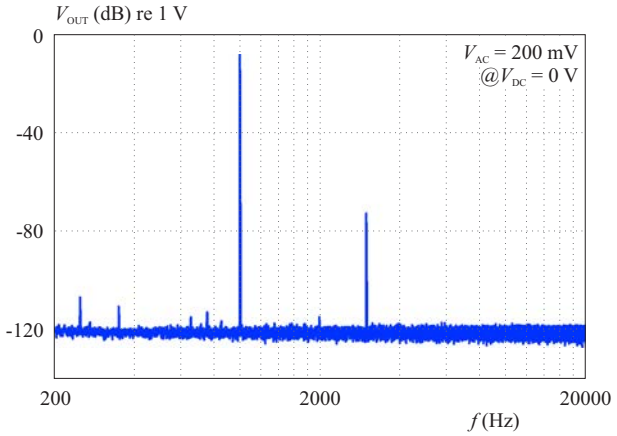

Fig. 10. FFT analysis of the emulator output signal for $V_{\mathrm{DC}} = 0$

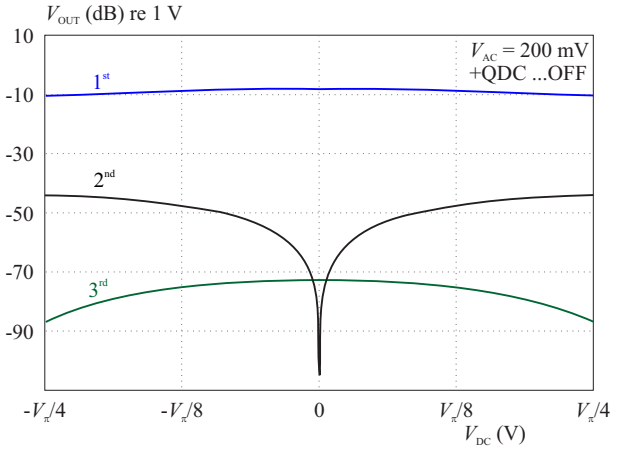

Fig. 11. Dependence of magnitudes of 1st, 2nd and 3rd harmonics on the bias voltage measured at the output of the emulator for $V_{\mathrm{AC}} = 200$ mV (+ QDC block is disabled *ie* quad-point is in the middle of the V_{DC} span)

by Shift block. The voltage generated by the Shift block is buffered by Buff. block and delivered to the monitor output as V_{DC} level.

If necessary the circuits of the +QDC, DFB and TIA Ref. blocks can be disabled. This alternatively allows operation in the mode of no emulation of DC offset of the TIA output. The DC level V_{DC} (Shift block) can be controlled smoothly by means of 11-turns potentiometer. That allows emulation of the progressive drift of the modulator. Alternatively, there is a possibility to switch on the pre-set V_{DC} value abruptly *ie* in leap. This may be useful for crucial tests of the prospective bias controller. The G_{out} gain can be switched over from $1 \times (R_{\mathrm{TIA}} = 470\ \mathrm{k\Omega})$ to the regime of smooth regulation in range of 0.5 to 1.5. This brings capability to adjust the TIA gain in range from 235 kΩ to 705 kΩ. In case of activation of all the blocks, the transfer function of the emulator is

$$V_{\mathrm{out}} = G_{\mathrm{out}} \left[\psi \tanh \frac{|G_{\mathrm{in}}| V'}{2V_{\mathrm{T}}} + V_{\mathrm{DFB}} \right] + V_{\mathrm{TIAr}} \qquad (23)$$

$$\text{where:} \quad V' = V_{\mathrm{in}} + V_{\mathrm{off}} - V_{+\mathrm{QDC}} + V_{\mathrm{DC}}.$$

The AD8674 low noise operational amplifiers were used to design and implement the emulator core, current source, summing blocks, offset blocks, and buffer amplifier as well.

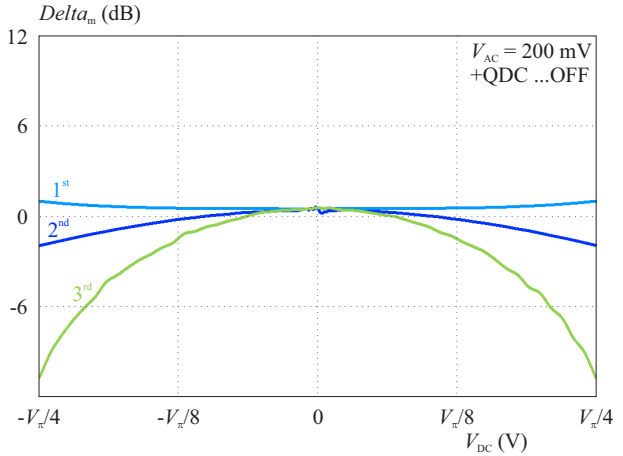

Fig. 12. Measured deviations of particular harmonics from theoretical values

6 Results

The emulator was verified by APX515 analyzer (Audio Precision corp.). The input of the device was driven by harmonic signal with frequency of 1 kHz and amplitude of $V_{\mathrm{AC}} = 200$ mV. The V_{DC} voltage (at the monitor output) was measured by Agilent 34401A.

The device was set to the state of emulation of quadrature point achievement. The chart in Fig. 10 reflects the measured spectrum at the output of the emulator. The FFT analysis was done with following set-up of the APX515: sampling rate 96 kSa/s, averaging 10, Hanning window. The measured data reveal very good signal to noise ratio and almost perfect suppression of 2nd harmonic. The THD at the output of the emulator is very low and is virtually formed by 3rd harmonic only. The value of 3rd harmonic reaches expected level. The presence of next higher harmonic components is negligible and in accordance with theory as well.

Then, there were measured levels of particular harmonics. Measured dependency of 1st, 2nd and 3rd harmonic ($V_{\mathrm{out1m}}, V_{\mathrm{out2m}}, V_{\mathrm{out3m}}$) on DC bias is in Fig. 11.

In detail, the emulator was measured for V_{DC} within the region $(-V_\pi/4; V_\pi/4)$ around the quadrature point.

The deviations of measured levels from theoretical values (10) and (11) for particular harmonics as a function of the DC bias are in Fig. 12.

Dependences of 1^{st} and 2^{nd} harmonics corresponds very good with theoretical assumptions considering the narrowed bias region $(-V_\pi/4; V_\pi/4)$. Error of emulation of 1^{st} harmonic is 0.5 dB at maximum. In case of 2^{nd} harmonic it is 2.5 dB. Error of emulation of the 3^{rd} harmonic is apparently higher. The most obvious it is at the margins of observed region where the error reaches up to 11.3 dB. Fortunately, the 3^{rd} harmonic has very low meaning (if any) for the feedback control of the modulator.

7 Conclusion

The level and the gradient of 2^{nd} harmonic can be used as an indicator for proper set-up and feedback control of bias voltage of MZM. This was validated by the derivations in the theory of the paper. Use of differential BJT stage to emulate behavior of a low-frequency-bias port of the MZM was proposed and demonstrated here. Nevertheless, the emulation has certain limits. The designed emulator is able to imitate the behavior of $1^{\mathrm{st}}, 2^{\mathrm{nd}}$ and 3^{rd} harmonics at the output of the real MZM in range of $(-V_\pi/4; V_\pi/4)$ around the quadrature point. Higher harmonics are under level of noise floor. The extensive suppression of the 2^{nd} harmonic can be observed in the middle of the range. The highest accuracy of the emulation is achieved in the middle of the range and in the close vicinity of the quadrature point. Of course, outside the observed range the emulator is not able to imitate the modulator with sufficient fidelity. On the other hand, this outside area is not significant for the feedback control. As the drift of real modulator is typically gradual and slow the range of $(-V_\pi/4; V_\pi/4)$ seems to be wide enough to keep the feedback loop safely locked. The designed device brings possibility to safely test and tune feedback control systems used for driving the bias voltage of MZM. As this activity can be done without the real modulator itself the risk of break or damage of an expensive and sensitive modulator is minimized.

Acknowledgements

This work was supported by the Ministry of Education, Youth and Sports of the Czech Republic under the RICE New Technologies and Concepts for Smart Industrial Systems, project No. LO1607.

References

[1] H. Nagata, K. Kiuchi and T. Saito, "Studies of Thermal Drift as a Source of Output Instabilities Ti: LiNbO3 Optical Modulators", *Journal of Appl. Physics*, vol. 75, no.9, pp. 4762-4764, 1994.

[2] J. P. Salvestrini, L. Guilbert, M. Fontana, M. Abarkan and S. Gille, "Analysis and Control of the DC Drift LiNbO", *Journal of Lightwave Technology*, vol. 29, no.10, pp. 1522-1534, 2011.

[3] J. Svarny, "Analysis of Quadrature Bias-point Drift of Mach-Zehnder Electro-optic Modulator", *Proc. Int. Conf. BEC2010*, Tallinn, Estonia, pp. 231-234, 2010.

[4] A. Chen and E. J. Murphy, *Broadband Optical Modulators - Science, Technology, and Applications*, CRC Press, 2012.

[5] C. H. Cox and E. I. Ackerman, "Modulator Bias Control", *U. S. Patent 7 369 290 B1*, 5/6/2008.

[6] E. I. Ackerman, H. Roussell and C. H. Cox, "Bias Controllers for External Modulators Fiber-Optic Systems", *Lightwave*, vol. 18, pp. 175-178, 2011.

[7] Y. Fu, X. Zhang, B. Hraimel, T. Liu, and D. Shen, "Mach-Zehnder: A Review of Bias Control Techniques for Mach-Zehnder Modulators Photonic Analog Links", *IEEE Microwave Magazine*, vol. 14, no.7, pp. 102-107, 2013.

[8] E. I. Ackerman and C. H. Cox, "Effect of Pilot Tone Based Modulator Bias Control on External Modulation Link Performance", *Proc. Int. Conf. MWP2000*, Oxford, UK, pp. 121-124, 2000.

[9] D. T. Bui and B. Journet, "Electro-Optic Modulator Bias Point Optimization by Detecting its Nonlinear Behavior", *Proc. Int. Conf. on Communications and Electronics*, Nha Trang, Vietnam, pp. 118-123, 2010.

[10] Y. Li, L. Yu and A. Lv, "Automatic Bias Control of Electro-optic Modulator Optical-fiber Brillouin Sensing System", *Proc. Int. Conf. ICADE2012*, Beijing, China, pp. 98-102, 2012.

[11] J. Svarny, "Implementation of a Precise Quadrature Point Bias Controller to the Integrated Intensity Electro-optic Modulator", *Proc. Int. Conf. BEC2012*, Tallinn, Estonia, pp. 136-136, 2012.

[12] C. J. Paull and W. A. Ewans, "Waveform Shaping Techniques for the Design of Signal Sources", *Radio and Electronic Engineer*, vol. 44, no.10, pp. 523-532, 1974.

[13] AN-263 Sin Wave Generation Techniques Texas Instruments Application Note, SNOA655C, Dallas, Texas U.S., 2013, http://www.ti.com/lit/an/snoa665c/snoa665c.pdf.

[14] R. G. Meyer, W. M. C. Sansen, S. Lui and S. Peeters, "The Differential Pair as a Triangle-Sin Wave Converter", *IEEE Journal of Solid-State Circuits*, vol. 11, no.3, pp. 418-420, 1976.

[15] J. W. Fattaruso and R. G. Meyer, "Triangle to Sine Wave Conversion with MOS Technology", *IEEE Journal of Solid-State Circuits*, vol. 20, no.2, pp. 623-631, 1985.

[16] C. A. R. Filho, M. P. Pessatti and J. P. C. Cajueiro, "Analog Triangular-to-Sine Converter Using Latteral-pnp Transistors CMOS Process", *Proc. 9th International Conference on Electronics*, Circuits and Systems ICECS2002, Dubrovnik, Croatia, pp. 253-256, 2002.

[17] B. Gilbert, "Circuits for the Precise Synthesis of the Sine Function", *Electronics Letters*, vol. 13, no.17, pp. 506-508, 1977.

[18] T01 - Matched Monolitic Dual Transistor Analog Devices Data Sheet, D00282-0-9/14(D), Norwood, MA, U.S., 2014, http://www.analog.com/media/en/technical-documentation /data-sheets/MAT01.pdf.

Received 10 November 2017

Jiří Švarný received the MS and PhD degrees in electrical engineering from the University of West Bohemia (UWB), Pilsen, Czech Republic, in 1997 and 2000, respectively. In 2000, he joined the UWB as an Assistant Professor at the Department of Technologies and Measurement, Faculty of Electrical Engineering. Since 2011, he has been a R&D engineer at the Regional Innovation Centre for Electrical Engineering (RICE) which is one of research centers at UWB. His research activities are focused on design of specialized measuring electronic devices and systems including optoelectronic systems.